HHS Public Access

Author manuscript

Free Radic Res. Author manuscript; available in PMC 2021 May 22.

Published in final edited form as:

Free Radic Res. 2020 May ; 54(5): 319–329. doi:10.1080/10715762.2020.1763332.

Protective effects of tiopronin on oxidatively challenged human lung carcinoma cells (A549)

Justin Beltz[a,1], **Anna Chernatynskaya**[a,1], **Annalise Pfaff**[a], **Nuran Ercal**[a,*]

[a]Department of Chemistry, Missouri University of Science & Technology, Rolla, MO, USA

Abstract

Tiopronin (MPG) is a thiol antioxidant drug that has been explored as a treatment for various oxidative stress-related disorders. However, many of its antioxidant capabilities remain untested in well-validated cell models. To more thoroughly understand the action of this promising pharmaceutical compound against acute oxidative challenge, A549 human lung carcinoma cells were exposed to *tert*-butyl hydroperoxide (*t*BHP) and treated with MPG. Analyses of cell viability, intracellular glutathione (GSH) levels, and prevalence of reactive oxygen species (ROS) and mitochondrial superoxide were used to examine the effects of MPG on *t*BHP-challenged cells. MPG treatment suppressed intracellular ROS and mitochondrial superoxide and prevented *t*BHP-induced GSH depletion and apoptosis. These results indicate that MPG is effective at preserving redox homeostasis against acute oxidative insult in A549 cells if present at sufficient concentrations during exposure to oxidants such as *t*BHP. The effects of treatment gleaned from this study can inform experimental design for future *in vivo* work on the therapeutic potential of MPG.

Keywords

thiols; antioxidant; oxidative stress; reactive oxygen species (ROS); glutathione; tiopronin

Introduction

N-(2-mercaptopropionyl)glycine (MPG), or tiopronin, is low-molecular-weight thiol derivative of glycine that has been used to treat a variety of conditions. MPG was one of the first disease-modifying anti-rheumatic drugs [1–3], but it has been superseded by biologics and is now only applied in certain refractory cases [4,5]. MPG is the first-line treatment for cystinuria, in which it forms mixed disulfides that are up to 50 times more soluble than cystine, thus preventing the formation of cystine kidney stones [6,7]. While these applications fill important medicinal niches, the antioxidative properties of MPG have

*Corresponding author address: 230 Schrenk Hall, 400 W. 11th Street, Rolla, MO 65409, USA; nercal@mst.edu; phone: (573) 341 6950.

[1]J. Beltz and A. Chernatynskaya contributed equally to this work as primary authors.

Disclosure statement

The authors report no conflict of interest.

Data availability statement and data deposition

The data generated from the current study are available from the corresponding author on reasonable request.

warranted its investigation for the treatment of more prevalent conditions. Its -SH moiety can reduce disulfide linkages between oxidized biothiols, like glutathione disulfide, restoring them to their native state [8,9]. In addition, MPG is regarded as an effective chelator of heavy metals such as mercury and copper. *In silico* models predict that formation of MPG-copper(II) complexes can reduce the rate constant of the first step in the Haber-Weiss reaction six-fold [10]. Because of these significant antioxidant properties, MPG has been used to protect against chemotherapy-induced nephro- and hepatotoxicity [11,12], radiation poisoning [13], and ischemia-reperfusion injury to cardiac and lung tissue [12,14]. Further, MPG may be able to counteract oxidative processes that lead to lens opacification in senile cataracts [15–21]. MPG offers several advantages over similar drugs, including a more favorable side effect profile than D-penicillamine [4] and better bioavailability than *N*-acetylcysteine [22,23]. Moreover, MPG's primary metabolite, 2-mercaptopropionic acid, is also a potent radical scavenger [24]. With the growing impetus to repurpose pharmaceuticals, the medical community stands to gain potential treatments and greater understanding of oxidative stress-related conditions from renewed interest in MPG. However, its action against acute exogenous oxidative insult in cell models has not been thoroughly characterized.

To bridge this gap in understanding, well-established cell lines such as A549 are commonly used to study the action of drugs *in vitro* [25–27]. As a pulmonary epithelial cell line, it is often employed to study effects of inhalation exposure to environmental contaminants, in which oxidative stress plays a key role [28]. Further, it is recognized as a useful model for early-stage biopharmaceutical research, including studies of drug metabolism and cytotoxicity [29,30]. A well-validated oxidant is another integral component of an appropriate system for testing an antioxidant drug. For *in vitro* studies, *tert*-butyl hydroperoxide (*t*BHP) is more reliable than hydrogen peroxide, as *t*BHP has demonstrated more consistent ability to induce oxidative stress than H_2O_2 [31,32]. This may be attributed to the greater stability of the *tert*-butoxyl radical in aqueous solution [33] and fewer enzymes dedicated to its detoxification (e.g., glutathione peroxidase only versus glutathione peroxidase and catalase for H_2O_2) [25]. Further, decomposition of *t*BHP and downstream action of its byproducts may recapitulate many of the oxidative mechanisms observed *in vivo*, including lipid peroxidation, DNA damage, depletion of GSH and protein thiols, alteration of intracellular calcium homeostasis, and apoptosis [25,34]. For these reasons, *t*BHP is better suited for probing the intracellular action of MPG. Therefore, we utilized *t*BHP to rapidly induce severe oxidative damage in A549 cells and administered MPG simultaneously to test the action of MPG against acute oxidative insult. To observe and characterize the effects of MPG under these conditions, we examined cell viability, intracellular GSH levels, and distribution of cells in apoptotic and non-apoptotic populations exhibiting intracellular ROS and mitochondrial superoxide.

Materials and methods

Chemicals and reagents

MPG, *t*BHP solution, Tris-HCl, L-serine, boric acid, diethylenetriaminepentaacetic acid, and *N*-(1-pyrenyl)maleimide were purchased from MilliporeSigma (St. Louis, MO). MPG stock

solutions were prepared in sterile Type 1 water prepared in-house with a Millipore Simplicity 185 System. Glacial acetic acid, o-phosphoric acid, and high-performance liquid chromatography (HPLC) grade solvents were purchased from Fisher Scientific (Fair Lawn, NJ).

Cell culture and preliminary experiments

A549 (human lung carcinoma) cells were kindly provided by Dr. Yue-Wern Huang from the Biological Sciences Department at Missouri University of Science and Technology.

Cells were grown in phenol-red-free DMEM/F12 medium (Thermo Fisher Scientific, Waltham, MA) supplemented with 10% heat-inactivated fetal bovine serum (FBS) and 1% penicillin/streptomycin/amphotericin B (Thermo Fisher Scientific) in a humidified incubator with 5% CO_2/95% air at 37°C. Serum- and growth-factor-free medium was used for all MPG and *t*BHP experiments, instead of the fully supplemented media described above. Cells were passaged twice per week at a subcultivation ratio of 1:3. All experiments were performed using cells between passage 10 and 30.

To determine an appropriate concentration of *t*BHP for use in this study, A549 cells were seeded in multiple-well plates and divided into groups. Each group was incubated for 3 hours with a different concentration of *t*BHP in serum-free media, ranging from 0.25 mM to 4.0 mM. Cytotoxicity of *t*BHP in each group was assessed via MTT assay as described below to identify the range of concentrations at which cell viability was reduced to 50–60% of the control, which was shown to be 0.5 to 1.0 mM. To determine whether cells received sufficient oxidative insult, intracellular GSH levels were measured in groups treated with *t*BHP concentrations ranging from 0.4 to 0.8 mM for 3 hours. Based on these preliminary experiments, a concentration of 0.6 mM *t*BHP was selected for use in the remaining experiments.

Next, an appropriate concentration of MPG for treating *t*BHP-exposed cells was selected. To determine whether MPG alone had any adverse effect on cell viability, A549 cells were seeded in multiple-well plates and divided into groups. Each group was incubated for 3 hours with different concentrations of MPG in serum-free media, ranging from 0.08 mM to 10 mM, and MPG was not found to significantly affect cell viability at these concentrations (data not shown). To determine an appropriate concentration for use in *t*BHP-exposed cells, a similar experiment was conducted with the simultaneous addition of 0.6 mM *t*BHP and either 1.0, 1.5, 2.5, or 5.0 mM MPG for 3 hours. Cell viability and GSH levels in respective groups indicated that 5.0 mM MPG provided optimal protection against *t*BHP. Based on these preliminary experiments, 5.0 mM MPG and 0.6 mM *t*BHP were used in subsequent experiments to determine the effects of MPG on oxidative stress induced by *t*BHP.

Experimental Design

The A549 cells were grown in complete media and allowed to proliferate for 24 hours. The cells were divided into 4 treatment groups: control, MPG only, *t*BHP only, and MPG + *t*BHP. After the 24-hour proliferation time, the complete medium was removed and replaced with the treatment medium associated with the corresponding treatment group (Table 1). The treatment media were supplemented with *t*BHP or MPG immediately prior to each

experiment from freshly prepared concentrated stock solutions. The cells were allowed to incubate in the treatment media for 3 hours. After this time, the treatment media were removed. Cell viability and oxidative stress parameters including GSH and flow cytometric analysis of ROS and mitochondrial superoxide were determined after treatment as described in the following sections.

Cell viability

Cells were seeded at a density of 2×10^4 cells/well in 96-well plates and allowed to adhere and proliferate for 24 hours. Then, cells were divided into groups and treated as described in the experimental design. After the treatment, the treatment media were replaced with fresh F12 medium, and cell viability was determined using the Vybrant MTT Cell Proliferation Assay Kit (Invitrogen, Carlsbad, CA) as described by the manufacture. The MTT assay is a colorimetric assay through which cell viability is estimated by conversion of the water soluble MTT (3-(4,5-dimethylthiazol-2-yl)-2,5-dimethyltetrazolium bromide) to an insoluble formazan by viable cells. The formazan is then solubilized by sodium dodecyl sulfate (SDS), and the concentration is determined by measuring absorbance at 570 nm using a microplate reader (Fluor Star Optima, BMG, Labtech). Cell viability was expressed as the absorbance by the contents of a given well divided by that of the mean absorbance measured for the control group.

Quantification of intracellular GSH level

Cells were seeded at a density of 6×10^5 cells/well in 6-well plates 24 hours before the experimental treatment. Cells were treated as described in the experimental design. Following treatment, the cells were harvested with trypsin/EDTA and collected in 1.5 mL RINO tubes (Next Advance, Troy, NY, USA). The cell suspensions were centrifuged at 500 × *g* for 10 min at 4°C. The supernatants were removed, and the cells were resuspended in 1 mL aliquots of PBS to rinse away remaining media and extracellular GSH. This centrifugation and rinsing process was repeated. After rinsing, the cells were centrifuged again at 500 × *g* and resuspended in 250 μL aliquots of chilled serine-borate buffer (100 mM Tris-HCl, 5 mM L-serine, 10 mM boric acid, 1 mM diethylenetriaminepentaacetic acid, pH 7.0). A 100 μL scoop was used to add about 100 μL of zirconium oxide beads (0.5 mm diameter, Next Advance) to each of the cell suspensions. The cells were homogenized using a Bullet Blender Storm tissue homogenizer (Next Advance) at speed “8” for 3 min. After homogenization, the cells were immediately centrifuged at 5000 × *g* for 5 min at 4°C. Then, 100 μL aliquots of supernatant were collected from each RINO tube for analysis of GSH and total protein content.

Intracellular GSH levels were determined by HPLC with pre-column derivatization and fluorescence detection, according to a method developed in our laboratory [35]. Briefly, 50-μL aliquots of cell homogenate were diluted with 200 μL of serine-borate buffer. The samples were derivatized by the addition of 750 μL of *N*-(1-pyrenyl)maleimide (1 mM in acetonitrile). The samples were mixed and allowed to react for 5 min. After this time, 10 μL of 2 M HCl were added to stabilize the fluorescent adducts. Samples were filtered with 0.45 μm nylon membrane filters. Samples were injected onto an Orochem (Naperville, IL, USA) Reliasil ODS-1 column (4.6 mm i.d. × 250 mm) and eluted with a mobile phase consisting

of 70:30 (v/v) acetonitrile-water with 1 mL/L of o-phosphoric acid and 1 mL/L of glacial acetic acid, delivered at a flow rate of 1 mL/min. GSH levels were determined by using a calibration curve prepared from standards processed in parallel with the unknown samples.

The GSH levels were normalized to the amount of total protein present in each sample. Total protein levels were estimated using the Coomassie dye-binding method described by Bradford [36]. Bradford dye reagent (Bio-Rad, Hercules, CA, USA) was diluted five-fold in serine borate buffer, and 1 mL aliquots of the diluted dye reagent were added to 20 μL of diluted cell homogenate in cuvettes. The samples were left to incubate at room temperature for at least 5 min. The absorbance of 595 nm light was correlated to the total protein concentration using a calibration curve. Albumin from bovine serum was used to make calibration standards to estimate the protein content in the cell homogenates.

To account for differences in live cell populations between treatment groups, GSH levels were reported in nanomoles of GSH per milligram of protein (nmol/mg).

Flow cytometry analysis of apoptotic cells and intracellular ROS measurement

Intracellular ROS content was measured using the carboxy derivative of fluorescein, carboxy-H_2DCFDA (6-carboxy-2',7'-dichlorofluorescein diacetate, Molecular Probes, Invitrogen), due to its additional negative charges that enhance cellular retention [37]. Flow cytometry (BD Accuri C6, BD Biosciences, Ann Arbor, MI) was used to assess the distribution of cells that contained ROS (ROS+ cells) within apoptotic and non-apoptotic cell populations. Cells were seeded on 24-well plates (Corning) at a density of 2×10^5 cells/well, grown over 24 hours, divided into groups and dosed as described previously. Trypsinized cells were washed with PBS and re-suspended in 250 μL of PBS containing 10 μM carboxy-H_2DCFDA. After incubation for 30 minutes at 37°C, the cells were washed with annexin V binding buffer and stained with 7-AAD (7-aminoactinomycin D, BD Pharmingen) and Annexin V Alexa Fluor 647 Conjugate (Invitrogen) for 15 minutes at room temperature in the dark. The FL-1 channel (λ_{ex} = 488 nm and λ_{em} = 533 nm) was used for carboxy-H_2DCFDA, and the FL-3 channel (λ_{ex} = 533 nm and λ_{em} = 670 nm) was used for 7-AAD. Annexin V Alexa Fluor 647 fluorescence was measured using the FL-4 channel (λ_{ex} = 640 nm and λ_{em} = 675 nm). Debris were excluded by forward vs. side scatter gating. Results are reported as percent of total cell population.

Flow cytometry determination of mitochondrial superoxide

MitoSOX Red mitochondrial superoxide indicator (MSR) is a fluorogenic dye for selective detection of superoxide in mitochondria of live cells (Molecular Probes, Eugene, OR). MSR is a dihydroethidium dye with a lipophilic, positively-charged side-chain for targeted absorption by the mitochondria. Upon oxidation by superoxide, the dye exhibits red fluorescence [38]. For analysis of superoxide generated in mitochondria, cells were grown in the same conditions as for the measurement of ROS content via flow cytometer. Harvested cells were washed with PBS and re-suspended in 250 μL of PBS containing 5 μM MSR. Cells were incubated for 30 minutes at 37°C. After incubation with MSR, LIVE/DEAD Fixable Green Dye (Molecular Probes, Eugene, OR) was added directly to each sample according to the manufacture's recommendation. Cells were incubated for an additional 15

minutes at room temperature. The final stain, Annexin V Alexa Fluor 647 Conjugate, was added after washing cells with annexin V buffer. Cells were analyzed by flow cytometry using the FL-1 channel (λ_{ex} = 488 nm and λ_{em} = 533 nm) for LIVE/DEAD Fixable Green, the FL-2 channel for MSR (λ_{ex} = 488 nm and λ_{em} = 585 nm), and the FL-4 channel for Annexin-V Alexa Fluor 647 (λ_{ex} = 640 nm and λ_{ex} = 675 nm). Results are reported as percent of total cell population with MSR fluorescence (MSR+) cells in apoptotic and viable populations in each treatment group. Debris were excluded by forward vs. side scatter gating.

Statistical analysis

Statistical analysis was performed using GraphPad Prism 8 software (GraphPad, San Diego, CA, USA). All values were reported as mean ± standard deviation of at least three separate experiments, with n = 3–16. Statistical significance was performed by two-way analysis of variance (ANOVA) for flow cytometry experiments and one-way ANOVA for all other experiments. ANOVA was followed by Tukey's or Dunnette's multiple comparison tests.

Results and discussion

Selection of dosing concentrations

To determine an appropriate concentration of *t*BHP for inducing oxidative stress, cell viability and GSH levels were determined following exposure to varied concentrations of *t*BHP. GSH, γ-glutamyl-cysteinyl-glycine, is the most abundant non-protein thiol in the body and an essential endogenous antioxidant. It plays a vital role in reduction and detoxification of ROS, including peroxides like *t*BHP and is therefore crucial to the maintenance of redox homeostasis. Increase in oxidants can upset this delicate balance, leading to the oxidative modification of critical cellular components, dysfunction, and ultimately apoptosis. The effects of increasing *t*BHP concentrations on cell viability and GSH levels are reported in Figure 1. Concentrations from 0.25 mM to 4.0 mM significantly decreased cell viability in a dose-dependent manner. The effect of *t*BHP concentration on GSH levels and cell morphology were also considered for selection of an appropriate concentration of *t*BHP for subsequent experiments. *t*BHP concentrations from 0.4 mM to 0.8 mM resulted in a statistically significant decrease in levels of intracellular GSH, which correlates with the dose-dependent decrease in cell viability.

Upon comparing the effects of *t*BHP on GSH levels and cell morphology, it was noted that at 0.6 mM *t*BHP, GSH had decreased by approximately 50%, but at 0.8 mM, cells lost adhesion, which interfered with analysis and weakened integrity of the model overall. A *t*BHP concentration of 0.6 mM struck the best balance between oxidative damage and maintenance of normal cell morphology. Therefore, 0.6 mM *t*BHP was selected for subsequent experiments. Although this *t*BHP concentration is relatively high, the A549 cell line is reportedly resistant to oxidative insult [39].

In the next set of experiments, a variety of MPG concentrations from 1.0 to 5.0 mM were tested in different groups to determine the appropriate concentration for protection against oxidative stress induced by 0.6 mM *t*BHP. Intracellular GSH levels were used to assess the

effectiveness of each dose, and the results are shown in Figure 2. Concentrations ranging from 1.0 mM to 5.0 mM MPG afforded significant improvement in GSH levels compared to untreated, *t*BHP-exposed cells, but cells treated with 5.0 mM MPG exhibited the highest GSH levels. Since preliminary experiments showed concentrations of MPG up to 10 mM to be nontoxic to A549 cells, treatment with 5.0 mM MPG was deemed an appropriate treatment for *t*BHP-induced oxidative stress for the remainder of the study.

Effect of MPG on intracellular GSH in oxidatively challenged A549 cells

To confirm the effects of 5.0 mM MPG on intracellular GSH levels in A549 cells, the cells were divided into groups as discussed in the experimental design and seeded as described earlier. The results of the intracellular GSH analyses are reported in Figure 3A. The data were normalized by the amount of protein present in each sample to account for differences in viable cell count. Exposure to *t*BHP without MPG resulted in a significant decrease in intracellular GSH levels compared to the control group. Cells treated with MPG, either with or without *t*BHP, had GSH levels that were not significantly different from that of the control group. Therefore, administration of 5.0 mM MPG with 0.6 mM *t*BHP was effective for preventing loss of free GSH, and MPG alone does not increase GSH levels beyond that of the control group. These results are consistent with the hypothesis that GSH levels are spared by the action of MPG as opposed to being directly increased.

Effect of MPG on viability of oxidatively challenged A549 cells

To determine whether MPG could protect cells from *t*BHP-induced loss of viability, the MTT assay was used as an indicator of cellular metabolism. This assay is based on the ability of metabolically active cells to reduce MTT to an insoluble, colored formazan product that can be measured spectrophotometrically. Cell viability for each treatment group is reported in Figure 3B as a percentage of absorbance at 570 nm compared to that of the control group. As was the case in our preliminary studies, cells exposed to 0.6 mM *t*BHP without MPG exhibited significantly less viability compared to the cells in the control group, and the viability of cells in the MPG + *t*BHP group was statistically similar to that of the cells in the control group. Treatment of A549 with 5 mM MPG alone also did not increase or decrease cell viability.

This trend closely parallels that of intracellular GSH levels and makes sense in the context of the biochemistry behind the MTT assay. The reduction of MTT to formazan is sensitive to decreases in available NADPH [40]. The NADPH cofactor serves as the reductant for a host of anabolic processes, as well as the reduction of oxidized glutathione to its active reduced form. Thus, gross metabolic dysfunction resulting from *t*BHP is manifested in the inability of oxidatively damaged, dying cells to reduce MTT and regenerate GSH from its oxidized form. In contrast, cells treated with MPG exhibited marked improvement in both cell viability and GSH levels. We hypothesize that this is due to the following effects of MPG. As a thiol antioxidant that can directly reduce *t*BHP-derived ROS, MPG can spare GSH from oxidation, leaving cellular GSH stores largely intact. In preventing oxidation of GSH, MPG also preserves NADPH for use in reductive biosynthesis and conversion of MTT to formazan.

Effect of treatment on apoptotic and necrotic cell populations

Flow cytometry is a well-established technology that has been widely used for measuring intrinsic and extrinsic properties of fluorescently labeled cells. This property permits the identification of subpopulations within the sample, and quantification of cell populations through selective fluorescence labeling. While microplate readers provide rapid data acquisition, the accuracy of the measurements suffers since the end value corresponds to the average fluorescence per well while flow cytometry provides information at the single-cell level. For this analysis, cells were labeled with 7-AAD and Annexin V Alexa 647 to investigate live, necrotic, and apoptotic cell populations. Live cells are not typically permeable to 7-AAD. Cells in early apoptotic stages bind only to Annexin V Alexa 647, while cells in late apoptotic stages bind to both Annexin V Alexa 647 and 7-AAD. Necrotic cells bind to 7-AAD, but not Annexin V Alexa 647.

Representative dot-plots from the flow cytometry analysis are provided in Figure 4. The mean distributions of cells among apoptotic, necrotic, and viable cell populations from 8 replicate experiments are summarized in Table 2. As observed previously, the percentage of viable cells in the MPG + *t*BHP treated group was significantly higher than in the *t*BHP group. Further, the percentage of viable cells in the MPG + *t*BHP group was statistically similar to the percentages in the MPG only group and the control group. The same trend was observed within late apoptotic subpopulations. Exposure to 0.6 mM *t*BHP without MPG resulted in an elevated proportion of cells exhibiting fluoresence associated with binding of 7-AAD and Annexin V Alexa 647. However, cells treated with MPG, alone or with *t*BHP, were not significantly different from the control cells. These data suggest that exposure to 0.6 mM *t*BHP without MPG results in oxidative stress-associated apoptosis while treatment with MPG mitigates the damage that triggers this process.

Although there does not appear to be a significant difference in the proportion of cells occupying the necrotic quadrant among groups, this can be attributed to the fact that cellular debris are excluded prior to quantitation. There was a significantly lower number of cells available for counting in the *t*BHP only group, compared to the other groups. This loss of countable cells is indicative of membrane disintegration associated with *t*BHP exposure.

Distribution of cells with ROS present in apoptotic and non-aptoptotic subpopulations

Based on the results of GSH and MTT assays, we hypothesized that MPG prevents cell death by protecting cells from oxidative damage, and therefore, we would expect to see significantly higher levels of ROS in cells in the *t*BHP only group than in the other groups. To estimate the levels of intracellular ROS, carboxy-H_2DCFDA was used to identify ROS+ cells. Carboxy-H_2DCFDA is a membrane-permeable derivative of the fluorescent probe fluorescein. Upon cleavage of its acetate groups and oxidation by intracellular ROS, the dye becomes trapped within the cell and fluoresces green [38]. Cells were co-stained with two other fluorescent probes, Annexin V Alexa Fluor 647 conjugate and 7-AAD, and then the cells were subjected to flow cytometric analysis. Representative dot plots are shown in Figure 5. In this study, co-staining was used to differentiate between apoptotic and non-apoptotic cell subpopulations and to exclude necrotic cells since membrane leakage makes estimation of intracellular ROS unreliable. The results of the analysis (summarized in Table

3) indicate that there were indeed significantly more ROS detected in live cells treated with *t*BHP only than in any of the other groups. This correlates well with the GSH and cell viability results and is consistent with the supposition that MPG protects cells from oxidative stress by reducing ROS associated with exposure to *t*BHP.

Numbers of ROS+ cells in apoptotic subpopulations were low in all groups, and differences between these subpopulations did not reach statistical significance. Small subpopulations of apoptotic, ROS+ cells may be due to the exclusion of late-stage apoptotic and necrotic cells by gating out 7-AAD-fluorescent cells. As shown in Table 2, the *t*BHP only group had a significantly higher subpopulation of late-stage apoptotic cells, suggesting that *t*BHP-induces rapid progression to late-stage apoptosis or secondary necrosis [41]. Since these cells exhibit 7-AAD fluorescence, they would have been gated out and thereby excluded from the study [42].

Distribution of superoxide present in mitochondria of apoptotic and non-apoptotic populations

Low levels of superoxide in mitochondria are generated as a result of normal metabolic processes, but excessive amounts are associated with electron-transport chain dysfunction [43]. This can lead to decreased ATP production, loss of mitochondrial membrane potential, and ultimately opening of the mitochondrial permeability transition pore and initiation of the apoptotic cascade [44,45]. In this way, mitochondria are highly sensitive to fluctuations in redox status, [44] and may serve as a predictor of apoptotic response to acute oxidative insult [45].

MSR, a mitochondria-permeable dye, fluoresces upon oxidation by superoxide. Similar to the flow cytometric analysis of ROS+ cells, MSR was used to determine the percentage of cells with superoxide present in the mitochondria. Representative dot plots are shown in Figure 6. Table 4 shows the quantitative results as mean percentages of the total cell population. The percentage of MSR+ live cells in the MPG + *t*BHP group was significantly decreased compared to that in the *t*BHP only group. This indicates that MPG was able to preserve mitochondrial redox status. In light of the cell viability and GSH results, it may be the case that MPG prevents downstream release of mitochondria-derived ROS into the cell and halts progression towards apoptosis.

Conclusions

In this study, *t*BHP was used to induce oxidative stress in A549 cells. Cells exposed to 0.6 mM *t*BHP without MPG showed elevated levels of intracellular ROS, mitochondrial superoxide, and cell death while also showing reduced levels of the vital antioxidant GSH and reduced cell viability. When 5.0 mM MPG was present along with 0.6 mM *t*BHP, normal levels of these oxidative stress parameters were maintained. It is likely that MPG is interacting as a direct ROS scavenger, and the results obtained through this study suggest that if MPG is present in sufficiently high concentrations during an oxidative insult, it can be highly effective at preventing the ensuing damage. It is probable that the MPG reacts directly with *t*BHP in the treatment medium, reducing it and its oxidative byproducts before they can cause significant damage to the cells. This action is desirable for treatment applications

which demand protection against acute oxidative insult such as radioprotection, but it is important to consider the dosing conditions and timing since biological systems are inherently dynamic. This *in vitro* system lacks many of the complexities of *in vivo* models and is therefore subject to some limitations. Due to the robust nature of this lung carcinoma cell line, a relatively high dose of *t*BHP was required to model acute oxidative stress. Despite the popularity of this approach, it may not directly translate to *in vivo* systems. Thus, the results of this study warrant further investigation in more representative models, such as primary cell cultures and eventually animal studies.

Acknowledgements

The authors would like to thank Alex Cristea for his assistance in conducting preliminary work and GSH analysis.

Funding details

This work was supported by the Richard K. Vitek/FCR Endowment Missouri University of Science and Technology and the NEI of the National Institutes of Health under award number R15EY029813. The content is solely the responsibility of the authors and does not necessarily represent the official views of the National Institutes of Health.

References

1. Wood PL, Khan MA, Moskal JR. Mechanism of action of the disease-modifying anti-arthritic thiol agents D-penicillamine and sodium aurothiomalate: restoration of cellular free thiols and sequestration of reactive aldehydes. Eur J Pharmacol. 2008 2 2;580(1–2):48–54. [PubMed: 18022616]
2. Pasero G, Pellegrini P, Ambanelli U, et al. Controlled multicenter trial of tiopronin and D-penicillamine for rheumatoid arthritis. Arthritis Rheum. 1982 8;25(8):923–9. [PubMed: 7115451]
3. Amor B, Mery C, Gery AD. Tiopronin (N-[2-mercaptopropionyl] glycine) in rheumatoid arthritis. Arthritis Rheum. 1982;25(6):698–703. [PubMed: 7046758]
4. Jaffe IA. Adverse effects profile of sulfhydryl compounds in man. Am J Med. 1986 3;80(3):471–6. [PubMed: 2937293]
5. Czlonkowska A, Litwin T. Wilson disease - currently used anticopper therapy. Handb Clin Neurol. 2017;142:181–191. [PubMed: 28433101]
6. Fjellstedt E, Denneberg T, Jeppsson J-O, et al. Cystine analyses of separate day and night urine as a basis for the management of patients with homozygous cystinuria. Urol Res. 2001;29(5):303–310. [PubMed: 11762791]
7. Joly D, Rieu P, Mejean A, et al. Treatment of cystinuria. Pediatr Nephrol. 1999 11;13(9):945–50. [PubMed: 10603157]
8. Okumura S, Toshioka N, Asakura S, et al. Studies on the oxidation-reduction potentials of 2-mercaptopropionylglycine and penicillamine using thiol-disulfide exchange reactions with cysteine and glutathione. Yakugaku Zasshi. 1974;94(6):655–659. [PubMed: 4472644]
9. Wood PL, Khan MA, Moskal JR. Cellular thiol pools are responsible for sequestration of cytotoxic reactive aldehydes: central role of free cysteine and cysteamine. Brain Res. 2007 7 16;1158:158–63. [PubMed: 17555724]
10. Castañeda-Arriaga R, Vivier-Bunge A, Raul Alvarez-Idaboy J. Primary antioxidant and metal-binding effects of tiopronin: A theoretical investigation of its action mechanism. Comput Theor Chem. 2016;1077:48–57.
11. Zhang JG, Lindup WE. Tiopronin protects against the nephrotoxicity of cisplatin in rat renal cortical slices in vitro. Toxicol Appl Pharmacol. 1996 12;141(2):425–33. [PubMed: 8975767]
12. Atmaca G Antioxidant effects of sulfur-containing amino acids. Yonsei Med J. 2004 10 31;45(5):776–88. [PubMed: 15515186]

13. Devi PU, Saharan BR. Chemical protection of mouse spermatocytes against gamma-rays with 2-mercaptopropionylglycine. Experientia. 1978 1 15;34(1):91–2. [PubMed: 620750]
14. Date M-o, Morita T, Yamashita N, et al. The antioxidant N-2-mercaptopropionyl glycine attenuates left ventricular hypertrophy in in vivo murine pressure-overload model. J Am Coll Cardiol. 2002;39(5):907–912. [PubMed: 11869860]
15. Abdelkader H, Alany RG, Pierscionek B. Age-related cataract and drug therapy: opportunities and challenges for topical antioxidant delivery to the lens. J Pharm Pharmacol. 2015 4;67(4):537–50. [PubMed: 25643848]
16. Peng Y-S, Zhang J, Zhao W-J, et al. Inhibitory effect of tiopronin on hydrogen dioxide induced cataract in rabbit. Yanke Xinjinzhan. 2009 2;29(2).
17. Kobayashi S, Kasuya M, Ishii Y, et al. Effects of 2-mercaptopropionylglycine on the development of X-ray-induced cataract in rats. Curr Eye Res. 1992 11;11(11):1099–103. [PubMed: 1483339]
18. Ichikawa H, Imaizumi K, Tazawa Y, et al. Effect of tiopronin on senile cataracts. A double-blind clinical study. Ophthalmologica. 1980;180(5):293–8. [PubMed: 7010262]
19. Nishigori H, Hayashi R, Lee JW, et al. Effect of MPG on glucocorticoid-induced cataract formation in developing chick embryo. Invest Ophthalmol Vis Sci. 1984 9;25(9):1051–5. [PubMed: 6469489]
20. Jiang T-Y, Sun C-S, Shen X, et al. Development of a poloxamer analogs/bioadhesive polymers-based in situ gelling ophthalmic delivery system for tiopronin. J Appl Polym Sci. 2009;114(2):775–783.
21. Kuck JF Jr., Kuck KD. The Emory mouse cataract: the effects on cataractogenesis of alpha-tocopherol, penicillamine, triethylenetetramine, and mercaptopropionylglycine. J Ocul Pharmacol. 1988 Fall;4(3):243–51. [PubMed: 3198985]
22. Olsson B, Johansson M, Gabrielsson J, et al. Pharmacokinetics and bioavailability of reduced and oxidized N-acetylcysteine. Eur J Clin Pharmacol. 1988;34(1):77–82. [PubMed: 3360052]
23. Carlsson MS, Denneberg T, Emanuelsson BM, et al. Pharmacokinetics of oral tiopronin. Eur J Clin Pharmacol. 1993;45(1):79–84. [PubMed: 8405034]
24. Beltz J, Pfaff A, Ercal N. Simultaneous determination of tiopronin and its primary metabolite in plasma and ocular tissues by HPLC. Biomed Chromatogr. 2018 9 3:e4375.
25. Alia M, Ramos S, Mateos R, et al. Response of the antioxidant defense system to tert-butyl hydroperoxide and hydrogen peroxide in a human hepatoma cell line (HepG2). J Biochem Mol Toxicol. 2005;19(2):119–28. [PubMed: 15849717]
26. Unger RE, Pohl C, Hermanns I, et al. Cell culture systems for studying biomaterial interactions with biological barriers Methods of Analysis. Comprehensive Biomaterials. Vol. 1: Elsevier; 2011.
27. Ehrhardt C, Laue M, Kim K-J. In vitro models of the alveolar epithelial barrier In: Ehrhardt C, Kim K-J, editors. Drug Absorption Studies: In Situ, In Vitro And In Silico Models. Biotechnology: Pharmaceutical Aspects: Springer US; 2008.
28. Hsu HT, Tseng YT, Wong WJ, et al. Resveratrol prevents nanoparticles-induced inflammation and oxidative stress via downregulation of PKC-alpha and NADPH oxidase in lung epithelial A549 cells. BMC Complement Altern Med. 2018 7 9;18(1):211. [PubMed: 29986680]
29. Buckley ST, Kim K-J, Ehrhardt C. In vitro cell culture models for evaluating controlled release pulmonary drug delivery In: Smyth HDC, Hickey AJ, editors. Controlled Pulmonary Drug Delivery. Advances in Delivery Science and Technology: Springer-Verlag New York; 2011.
30. Constant S, Wiszniewski L, Huang S. The use of in vitro 3D cell models of human airway epithelia (MucilAir(TM)) in inhalation technology In: Haycock JW, Ahluwalia A, Wilkinson JM, editors. Cellular In Vitro Testing: Methods and Protocols: CRC Press, Taylor & Francis Group; 2014.
31. Walther UI, Stets R. Glucocorticoid pretreatment increases toxicity due to peroxides in alveolar epithelial-like cell lines. Toxicology. 2009;256(1–2):48–52. [PubMed: 19056457]
32. Dierickx PJ, Van Nuffel G, Alvarez I. Glutathione protection against hydrogen peroxide, tert-butyl hydroperoxide and diamide cytotoxicity in rat hepatoma-derived Fa32 cells. Hum Exp Toxicol. 1999;18(10):627–633. [PubMed: 10557015]
33. Pryor Wa. OXY-RADICALS AND RELATED and Reactions. Annu Rev Physiol. 1986;48:657–667. [PubMed: 3010829]

34. Altman SA, Zastawny TH, Randers L, et al. tert.-butyl hydroperoxide-mediated DNA base damage in cultured mammalian cells. Mutat Res. 1994 4 1;306(1):35–44. [PubMed: 7512201]
35. Ates B, Ercal BC, Manda K, et al. Determination of glutathione disulfide levels in biological samples using thiol-disulfide exchanging agent, dithiothreitol. Biomed Chromatogr. 2009 2;23(2):119–23. [PubMed: 18646192]
36. Bradford MM. A rapid and sensitive method for the quantitation of microgram quantities of protein utilizing the principle of protein-dye binding. Anal Biochem. 1976 5 7;72:248–54. [PubMed: 942051]
37. Wang H, Joseph JA. Quantifying cellular oxidative stress by dichlorofluorescein assay using microplate reader. Free Radic Biol Med. 1999;27(5–6):612–616. [PubMed: 10490282]
38. Wojtala A, Bonora M, Malinska D, et al. Methods to monitor ROS production by fluorescence microscopy and fluorometry. Methods Enzymol. 2014;542:243–62. [PubMed: 24862270]
39. Baker MA, He S. Elaboration of cellular DNA breaks by hydroperoxides. Free Radic Biol Med. 1991;11(6):563–572. [PubMed: 1778502]
40. Vistica DT, Skehan P, Scudiero D, et al. Tetrazolium-based assays for cellular viability: a critical examination of selected parameters affecting formazan production. Cancer Res. 1991 5 15;51(10):2515–20. [PubMed: 2021931]
41. Zhang Y, Chen X, Gueydan C, et al. Plasma membrane changes during programmed cell deaths. Cell Res. 2018 1;28(1):9–21. [PubMed: 29076500]
42. Wlodkowic D, Telford W, Skommer J, et al. Apoptosis and beyond: cytometry in studies of programmed cell death. Methods Cell Biol. 2011;103:55–98. [PubMed: 21722800]
43. Gutteridge JMC, Halliwell B. Free Radicals in Biology and Medicine Oxford University Press; 2015.
44. Park J, Lee J, Choi C. Mitochondrial network determines intracellular ROS dynamics and sensitivity to oxidative stress through switching inter-mitochondrial messengers. PLoS One. 2011;6(8):e23211. [PubMed: 21829717]
45. Kroemer G, Galluzzi L, Brenner C. Mitochondrial membrane permeabilization in cell death. Physiol Rev. 2007 1;87(1):99–163. [PubMed: 17237344]

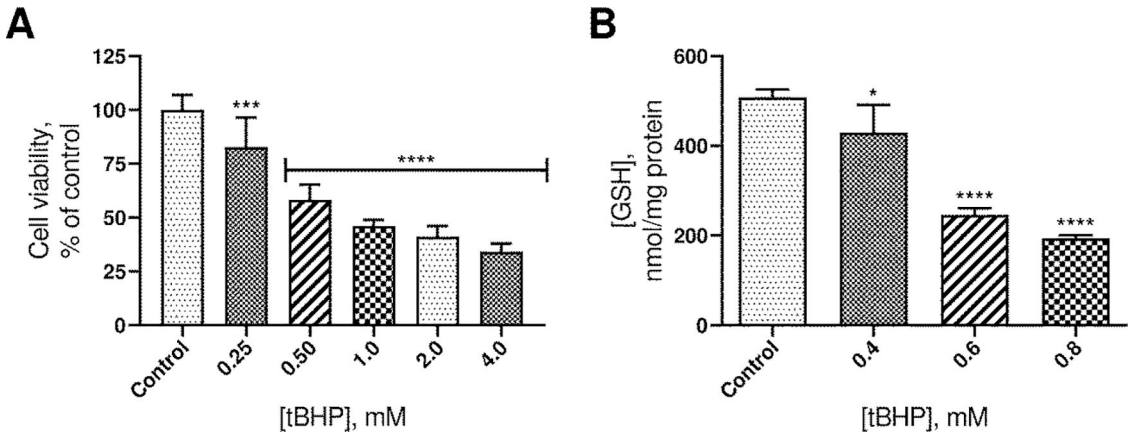

Figure 1.

A. Plot of cell viability vs. tBHP concentration. The height of the columns indicates the mean viability from 9 experiments. Error bars indicate standard deviation. B. Plot of intracellular GSH concentration vs. tBHP concentration. The height of the columns represents the mean of 3 experiments. Error bars indicate standard deviation. ****$p \leq 0.0001$ compared to control. ***$p \leq 0.001$ compared to control. *$p \leq 0.05$ compared to control.

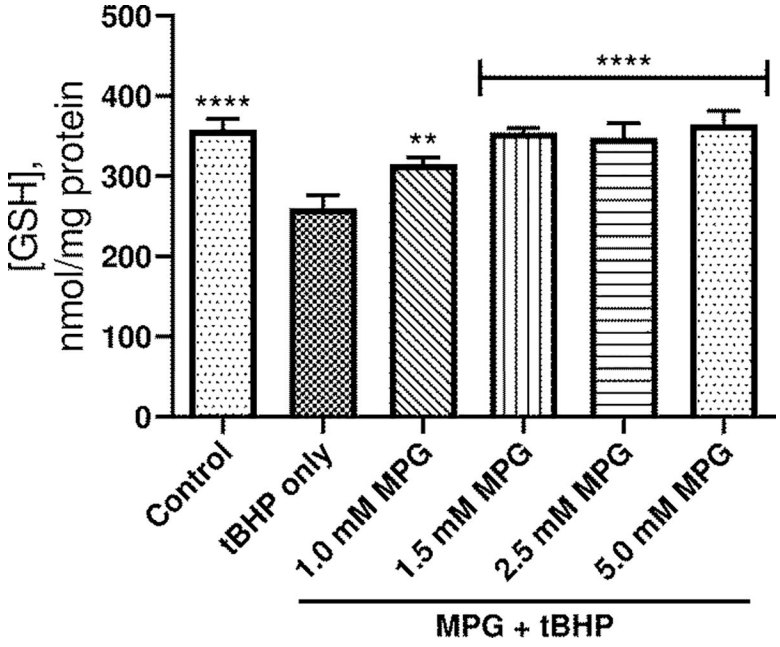

Figure 2.

Plot of intracellular GSH concentration vs. dosing concentration of MPG. The height of the columns represents the mean of 3 experiments. Error bars indicate standard deviation. ****p ≤ 0.0001 compared to tBHP only. **p ≤ 0.01 compared to tBHP only.

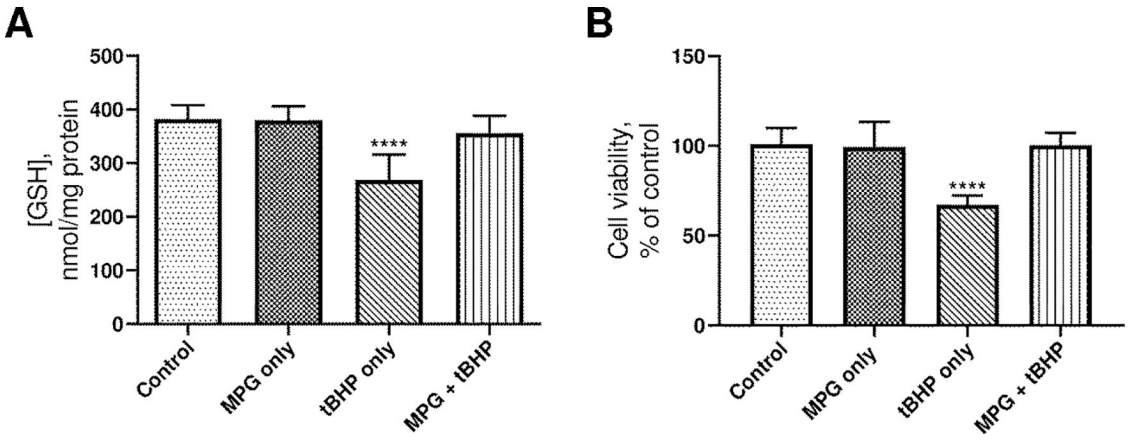

Figure 3.

A. Plot of intracellular GSH concentration vs. treatment. The height of the columns indicates the mean of 9 experiments, and error bars represent the standard deviation. B. Plot of cell viability vs. treatment. The height of the columns indicates the mean of 14 experiments, and error bars represent the standard deviation. ****$p \leq 0.0001$ compared to control.

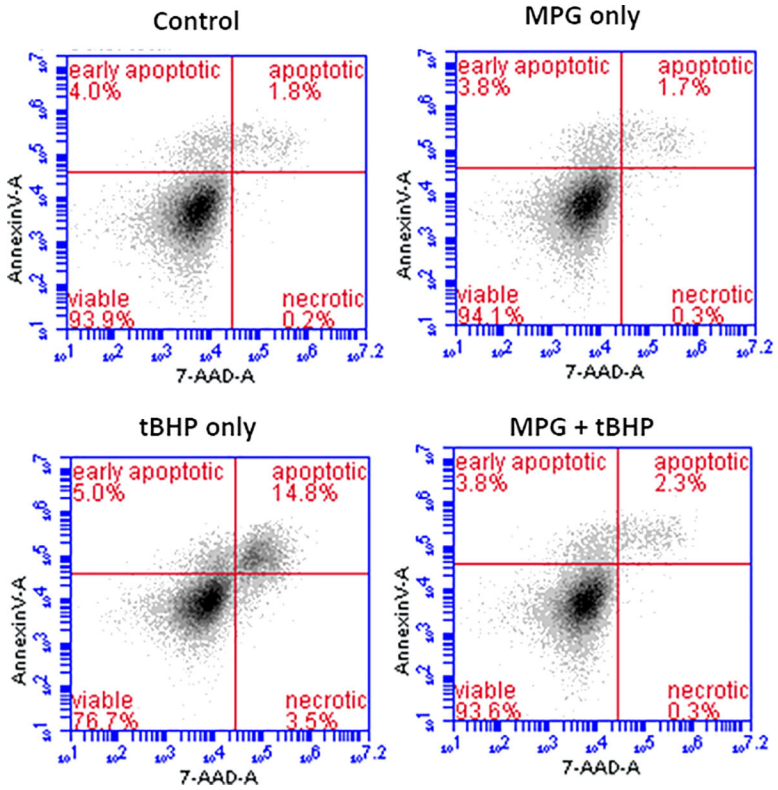

Figure 4.

Representative dot-plots from flow cytometry analysis of apoptotic cells. Show are plots of fluorescence associated with Annexin V Alexa 647 (FL-4) vs. 7-AAD (FL-3) from different treatment groups.

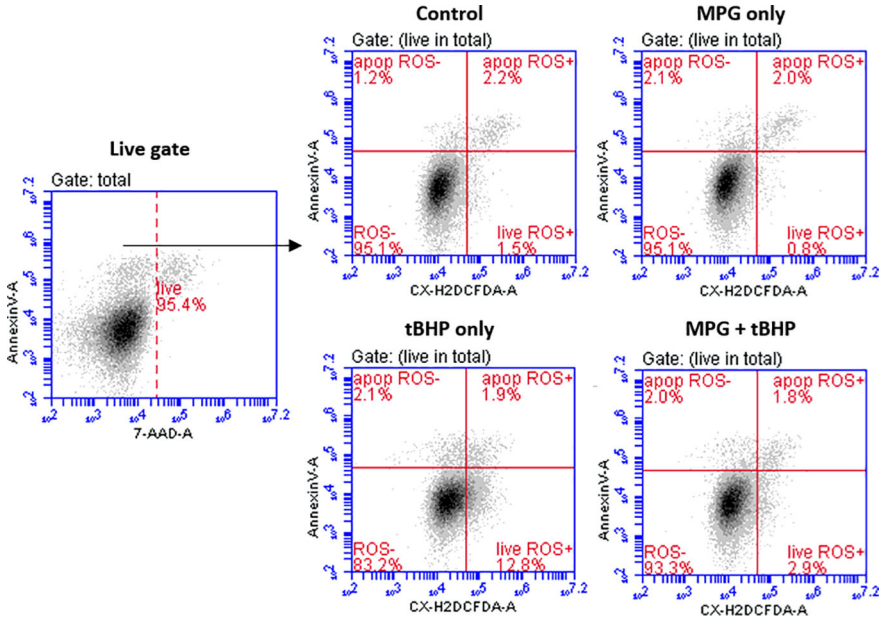

Figure 5.

Representative dot-plots from flow cytometry analysis of ROS in apoptotic and live subpopulations. The cells were gated to exclude debris. Viable cells were gated by exclusion of 7-AAD+ cells (FL-3) on 2D plots (live gate). The quantification of ROS was done using 2D plots of Annexin V Alexa 647 (FL-4) vs. Carboxy-H2DCFDA (FL-1).

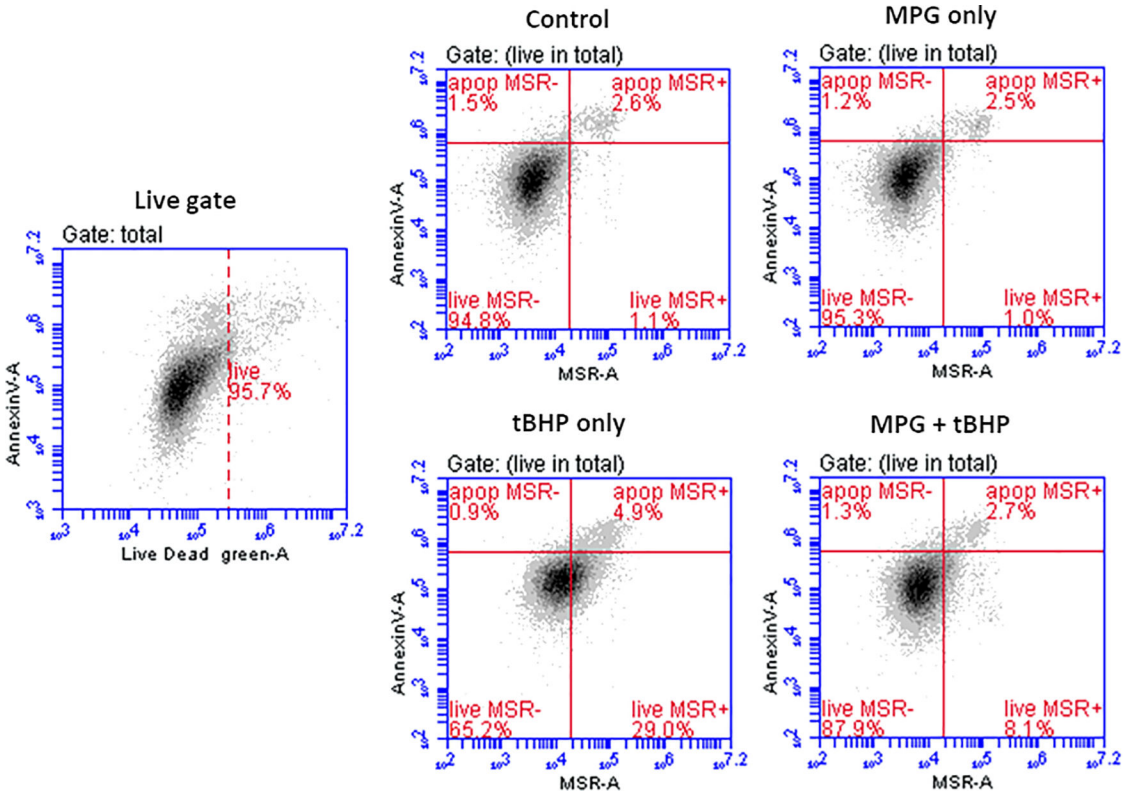

Figure 6.

Representative dot-plots of from flow cytometry analysis of superoxide in mitochondria. The total cells were gated to exclude debris. Viable cells were gated by exclusion of Live/Dead Green+ cells (FL-1) on 2D plots (live gate). The quantification of MSR+ cells was done using 2D plots of Annexin V Alexa 647 (FL-4) vs. MSR (FL-2).

Table 1.

Treatment media compositions

Group	Treatment medium
Control	Medium
MPG only	Medium + 5 mM MPG
*t*BHP only	Medium + 0.6 mM *t*BHP
MPG + *t*BHP	Medium + 5 mM MPG + 0.6 mM *t*BHP

Table 2.

Effects of exposure to *t*BHP and treatment with MPG on viable, apoptotic, and necrotic subpopulations.

Subpopulation	Cells in subpopulation (% of total cell population)†			
	Control	**MPG only**	***t*BHP only**	**MPG + *t*BHP**
Early apoptotic	3.1 ± 1.3	2.6 ± 0.9	4.3 ± 1.3	3.0 ± 0.7
Late apoptotic	2.3 ± 0.4****	2.3 ± 0.6****	11.2 ± 4.7	2.9 ± 0.7****
Viable	94.3 ± 1.2****	94.5 ± 0.8****	81.7 ± 8.2	93.5 ± 1.0****
Necrotic	0.4 ± 0.3	0.6 ± 0.4	2.8 ± 2.6	0.6 ± 0.6

† Mean ± SD of 8 experiments.

**** $p \leq 0.0001$, compared to *t*BHP only group.

Table 3.

Effects of *t*BHP exposure and MPG treatment on percentage of ROS+ cells in apoptotic and live cell populations.

Subpopulation	Cells in subpopulation (% of total cell population)[†]			
	Control	**MPG only**	***t*BHP only**	**MPG + *t*BHP**
ROS in apoptotic cells	1.7 ± 0.9	1.3 ± 0.8	3.6 ± 1.4	1.6 ± 0.6
ROS in live cells	1.5 ± 0.5 ****	2.2 ± 1.1 ****	22.5 ± 2.3	4.2 ± 1.0 ****
Total ROS	3.3 ± 0.9 ****	3.5 ± 1.6 ****	26.1 ± 2.7	5.8 ± 1.1 ****

[†]Mean ± SD of 8 experiments.

**** $p \leq 0.0001$, compared to *t*BHP only group.

Table 4.

Effects of exposure to *t*BHP and MPG on the percentage of MSR+ cells in apoptotic and live cell populations.

Subpopulation	Cells in subpopulation (% of total cell population)†			
	Control	MPG only	tBHP only	MPG + tBHP
MSR+ in apoptotic cells	2.1 ± 0.5	2.0 ± 0.4	3.9 ± 1.3	2.3 ± 0.5
MSR+ in live cells	1.2 ± 0.4****	1.3 ± 0.3****	24.3 ± 3.2	8.6 ± 1.9****
Total MSR+ cells	3.2 ± 0.8****	3.5 ± 0.5****	28.2 ± 3.5	10.9 ± 2.2****

†Mean ± SD of 8 experiments.

**** $p \leq 0.0001$, compared to *t*BHP only group.